Limnol. Oceanogr., 49(6), 2004, 1937–1948

Sinking behavior of gastropod larvae (*Ilyanassa obsoleta*) in turbulence

Heidi L. Fuchs,[1] *Lauren S. Mullineaux, and Andrew R. Solow*
Woods Hole Oceanographic Institution, Woods Hole, Massachusetts 02543

Abstract

Larvae of coastal gastropods sink in turbulence and may use nearshore turbulence as an initial settlement cue. Our objective was to quantify the relationship between turbulence and the proportion of sinking larvae for competent mud snail veligers (*Ilyanassa obsoleta*). We exposed larvae to a range of field-relevant turbulence conditions ($\varepsilon = 8.1 \times 10^{-3}$ to 2.7×10^{0} cm^2 s^{-3}) in a grid-stirred tank, holding other factors constant. We used a video plankton recorder to record larval movements in still water and in turbulence. Larval trajectories and velocity measurements were extracted using video-image analysis. We also measured turbulent flow velocities independently, using laser Doppler velocimetry. To interpret empirical measurements in terms of larval behavior, we developed a three-component, normal mixture model for vertical velocity distributions of larvae in turbulence. The model was fitted to observed larval velocities by maximum likelihood, to estimate the proportions of sinking, hovering, and swimming larvae. Over the range of turbulence intensities found in typical coastal habitats, the proportion of sinking larvae increased exponentially ($r^2 = 0.89$) with the log of the turbulence dissipation rate. The net mean behavioral velocity of the larvae shifted from positive to negative when the dissipation rate reached $\sim 10^{-1}$ cm^2 s^{-3}. By sinking when they enter turbulent, shallow water, competent larvae could improve their chances of settling in favorable coastal habitats.

Very little is known about how larval behavior in the plankton affects patterns of larval supply and settlement of benthic invertebrates. Much work has been done to describe larval behavior during the exploration of substrates, when larvae can sometimes select settlement sites over small scales (millimeters to centimeters). Less progress has been made on understanding the behavioral contribution while larvae are transported through the water column to benthic habitats. Under some hydrodynamic conditions, larvae could settle more successfully if they responded to waterborne cues by sinking toward the benthos. If the swimming velocity and gravitational sinking velocity differ by a factor of two or more, behavioral changes can significantly affect larval sinking fluxes (Gross et al. 1992; Eckman et al. 1994) and the time it takes for larvae to reach the bottom (McNair et al. 1997). Yet, with a few exceptions (e.g., Pawlik and Butman 1993; Tamburri et al. 1996; Welch and Forward 2001), it is unknown whether larvae change their behavior in response to conditions in the water column.

Ciliated larvae are generally assumed to reach the bottom boundary layer as passive particles (Butman 1987; Abelson and Denny 1997), but passive deposition alone cannot explain some population distributions. In Barnstable Harbor, Massachusetts, mud snails (*Ilyanassa obsoleta*) are the most conspicuously abundant megafauna on the intertidal mud flats, yet their settlement in the harbor seems improbable, because swimming larvae have mean upward velocities (H. L. Fuchs unpubl. data). Although swimming larvae are unlikely to be deposited on the bottom, sinking larvae have a good chance of settling along with fine sand in the harbor, and a behavioral switch may explain the apparently successful settlement of mud snail larvae.

With heavy shells for ballast, gastropod larvae can alter their vertical flux by changing their mode of behavior from swimming to sinking. Veligers are weak, ciliary swimmers with dense shells, and their gravitational sinking velocities are greater in magnitude than their maximum swimming velocities in any direction (e.g., Hidu and Haskin 1978). When larvae switch from swimming to sinking mode, the advective component of vertical flux changes accordingly. Most settlement models assume a constant larval velocity, ignoring possible effects of behavioral changes on larval fluxes (but see Eckman et al. 1994). Yet laboratory observations (Crisp 1984; Young 1995) and field evidence (Barile et al. 1994) suggest that gastropod larvae pull in their velums and sink when disturbed, and this behavioral change may affect settlement dynamics.

Turbulence could provide an initial cue for larvae to sink and explore for settlement sites (Chia et al. 1981). Many larvae settle preferentially on particular sediments (Snel-

[1] Corresponding author (hfuchs@whoi.edu).

Acknowledgments

Y. Yamashita helped collect and culture the larvae. We are grateful to J. Sisson for assistance with LDV measurements and to J. H. Trowbridge for guidance on spectral analysis. B. Raubenheimer and E. A. Terray also gave advice on flow data analysis. We thank C. DiBacco for generously sharing his culturing expertise and supplies, V. R. Starczak for advising us on the experimental design, and S. P. McKenna for introducing us to the turbulence tank. S. M. Gallager provided video equipment, software, and advice on particle tracking. M. G. Neubert, R. S. Scheltema, S. M. Gallager, G. R. Flierl, and D. Grünbaum contributed to intellectual discussions. The tank was used by permission of W. R. McGillis. P. Alatalo, R. S. Scheltema, and M. R. Sengco loaned culturing equipment, and M. G. Neubert loaned a computer. D. M. Kulis supplied the algal stocks. S. E. Beaulieu, F. J. Tapia, D. Grünbaum, R. Jennings, and two anonymous reviewers provided helpful comments on an earlier version of the manuscript.

The research was funded by a National Science Foundation graduate fellowship and a Woods Hole Oceanographic Institution Education fellowship to H.L.F. and a Woods Hole Oceanographic Institution Mellon Independent Study Award to L.S.M. and M. G. Neubert.

This is Woods Hole Oceanographic Institution contribution 11142.

Table 1. Representative dissipation rates for ocean regions.

Location	ε (cm^2 s^{-3})	Source
Open ocean (mixed layer)	10^{-7}–10^{-2}	Dillon and Caldwell (1980)
Continental shelf (mixed layer)	10^{-5}–10^{-2}	Oakey and Elliott (1982)
Tidal channels and estuaries	10^{-2}–10^{0}	Gross and Nowell (1985)
Surf zone	10^{-1}–10^{2}	George et al. (1994)

grove et al. 1998) or in the presence of conspecifics (Scheltema et al. 1981) or chemical cues (Pawlik 1992; Tamburri et al. 1996). However, preferred settlement sites can only be detected near the bottom and over small spatial scales (tens of centimeters). In shallow nearshore areas, sinking larvae would have more contact with the bottom and more settlement opportunities than swimming larvae. There would be no settlement-related benefits for larvae that sink in deeper, offshore areas, away from suitable habitats. Turbulence dissipation rates generally increase from offshore to inshore regions (Table 1) and might indicate to larvae when they are entering potential habitat areas. We hypothesize that turbulence above some threshold level provides a primary settlement cue for mud snail larvae and that larvae respond to this cue by sinking more frequently. This is a behaviorally mediated deposition hypothesis: larvae are deposited in nearshore environments because the behavioral response to a hydrodynamic cue increases their sinking fluxes in coastal areas.

We conducted larval behavioral experiments in a grid-stirred turbulence tank of the type used extensively in research on fluid turbulence (e.g., Hopfinger and Toly 1976; De Silva and Fernando 1994) and plankton feeding rates in turbulence (e.g., Saiz 1994; MacKenzie and Kiørboe 1995). Grid tanks are ideal for understanding larval behavior in water-column turbulence, because they lack a developed boundary layer and substrate-related settlement cues. Larvae are not induced to explore or attach to substrates in such tanks, and their observed activities are representative of behavior in the water column.

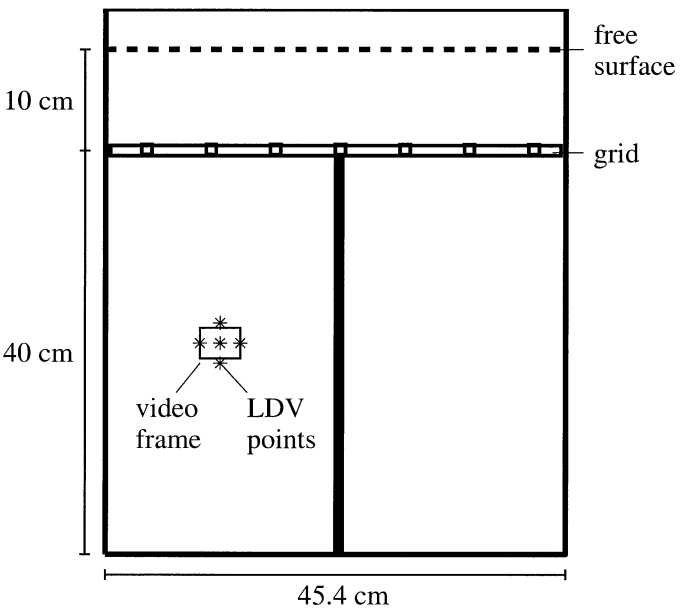

Fig. 1. Schematic of the turbulence tank as viewed from the side. The small rectangle indicates the location of video measurements, centered 19.1 cm from the bottom and 11 cm from the outer walls. Asterisks indicate the locations of LDV measurements.

Materials and methods

Larval cultures—Mud snail (*I. obsoleta*) egg capsules were collected at Barnstable Harbor on 30 June 2002 and divided into 12-liter buckets of filtered seawater in a 20°C culture room. Larvae hatched out over 10 d and were sieved daily into fresh culture buckets. Cultures were continually aerated, and seawater was changed every other day. The larvae were fed $\sim 10^5$ cells ml^{-1} of *Isochrysis galbana* and *Thalassiosira pseudonana.* Experiments were done in the culture room, so that larvae experienced consistent environmental conditions. Experiments began when larvae reached 24 d of age and were competent to metamorphose.

Turbulence tank—Our experiments were done in a 103-liter, grid-stirred turbulence tank (Fig. 1). The grid was centered at 40 cm from the bottom of the tank and 10 cm from the free surface, and was stirred from below with an oscillation amplitude of 11.34 cm. McKenna (2000) provides a detailed description of the tank. All measurements were made at a point far enough from the grid to be in an area of homogeneous, nearly isotropic turbulence (De Silva and Fernando 1994), and as far as possible from any boundaries. Turbulence intensity was proportional to grid oscillation frequency, which was controlled by setting the voltage. The turbulent Reynolds number Re_{HT} (*see Table 2 for a description of symbols*) was calculated as in Hopfinger and Toly (1976), with empirical constants given in McKenna (2000). Treatment levels were Re_{HT} = (100, 200, 300, 400, 500, 600), corresponding to the turbulence dissipation range expected in tidal inlets. In our measurement volume, there was a slight ($<$10 mm s^{-1}) downward mean flow due to the weak circulation generated by grid motion (McDougall 1979; McKenna 2000). Mean flow was accounted for in our analysis of larval behavior (see ''Analysis'' section).

Experimental design—Behavioral experiments were replicated six times with 24-d-old, competent larvae, and no larvae were reused. For the last replicate, only 27-d-old larvae were available. In each replicate, the turbulence tank was filled with 0.2 μm filtered seawater, at a temperature within $\pm$1°C of room temperature. Several thousand larvae were gently added to the tank, along with $\sim 2.5 \times 10^4$ cells ml^{-1} of food. Because of human error, no food was added in replicate 3.

Table 2. List of symbols. All velocities are vertical, with positive upwards.

Symbol	Description
ℓ	Eddy length scale
p_i	Probability density of w_L in mode i in still water
P	Total probability density of w_L in still water
p_{T^i}	Probability density of w_L in mode i in turbulence
P_T	Total probability density of w_L in turbulence
Re_{HT}	Theoretical turbulent Reynolds number
W_o	Flow velocity [$(\sim N(\mu_o, \sigma_o^2)$]
W_i	Larval behavioral velocity in mode i [$\sim N(\mu_i, \sigma_i^2)$]
W_{T^i}	Larval relative velocity in mode i [$(\sim N(\mu_{T^i}, \sigma_{T^i}^2)$]
w	Observed flow velocity
$\langle w \rangle$	Mean flow velocity ($=\mu_o$)
w_L	Observed larval velocity
$\langle w_L \rangle$	Net mean behavioral velocity
Δw_L	Behavioral velocity range
w'	RMS flow velocity from direct estimate
$\hat{w}'$	RMS flow velocity from spectral estimate ($\approx\hat{\sigma}_o$)
w'_{HT}	RMS flow velocity from empirical relationships
w'_{ML}	RMS flow velocity from maximum likelihood ($=\sigma_o$)
α_i	Proportion of larvae in mode i in still water
α_{T^i}	Proportion of larvae in mode i in turbulence
ε	Turbulence dissipation rate
η	Kolmogorov length scale
ν	Kinematic viscosity of seawater ($=0.01$ cm^2 s^{-1})
σ_n^2	Measurement noise variance

In each replicate, the larvae were exposed to alternating periods of calm water and turbulence (Fig. 2). After an initial acclimation period, video measurements were collected with no flow in the tank. Then six turbulence treatments were administered in a randomized sequence determined by a Latin square. Rest periods between treatments allowed larvae to regain their calm-water behavior. Video measurements were collected using an analog video plankton recorder. The video frame was 3 × 4 cm with an estimated 2-cm depth of field and was illuminated by an infrared spotlight (λ = 800 nm). Larvae were already acclimated to the ambient room lighting, so no light-related behavioral changes were expected during the experiments.

Before each replicate, a subsample of larvae was removed from the culture. Larval competency was verified by putting larvae in a petri dish with Barnstable Harbor sediment (Scheltema 1961); most stopped swimming and burrowed into the sediment within 3.5 h and metamorphosed within 24 h (n = 25). Other larvae were killed with a few drops of ethanol for fall-velocity measurements. Dead larvae with retracted velums were pipetted gently into the top of a 2-liter glass cylinder (45 cm tall, 7.7 cm diameter) filled with room-temperature seawater. Larvae were timed (n = 20) as they fell through a 12.5-cm distance near the bottom of the cylinder. We also anaesthetized larvae using $MgCl_2$ and attempted to measure their fall velocities with velums extended, but these larvae often recovered their mobility in the seawater column. Larval shell lengths were measured (n = 10) using a compound microscope with an optical micrometer.

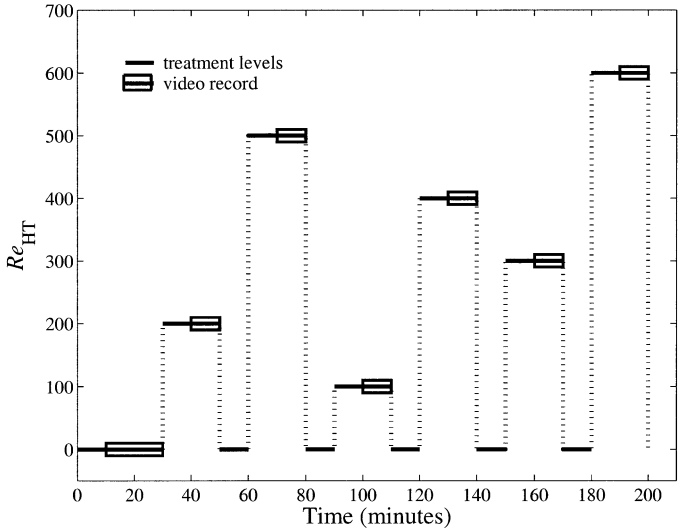

Fig. 2. Schematic of turbulent Reynolds number Re_{HT} vs. time in behavioral experiments. Turbulence became stationary in this tank after ~5 min of grid oscillation. Solid lines show the duration of each turbulence treatment, and rectangles indicate when the video record was taken. Rest periods are shown between turbulence treatments. This example is from replicate 1.

Flow velocity measurements—Flow velocities were measured with a Dantec two-axis laser Doppler velocimeter (LDV) after all larval experiments were completed, to avoid any interference of the laser or seeding particles with larval behavior. LDV is not ideal for turbulence measurements in near-zero mean flow (see ''Results'') but was the best instrument for measuring velocity remotely. The tank was filled with filtered seawater and heavily seeded with 10-μm hollow glass spheres (density = 1.05 g cm^{-3}). After 10 min of initial grid oscillation, vertical and horizontal velocities were measured (n = 2,000–10,000 records) by LDV at five points in the focal plane of the larval video frame (Fig. 1). Flow measurements were made at each turbulence treatment level in a randomized order and then were replicated for the center point only.

Larval velocity measurements—Larval video records were digitized using an EPIX PICXI SV5 image capture board with XCAP-Std software. Each 20-min still-water video segment was digitized into 40 50-frame sequences at 2 frames s^{-1} (fps). The turbulent video segments were digitized into 30 sequences per treatment replicate at 5 and 10 fps for $Re_{HT} \leq 200$ and $Re_{HT} > 200$, respectively. The sequence length was limited by image buffer size, and capture intervals were selected so that movements of individual larvae could be followed easily from frame to frame.

Image sequences were processed digitally, to measure the larval vertical velocities. Larval centroid positions were found using Matlab software (provided by S. M. Gallager) and linked into larval trajectories using a Matlab algorithm based on distance and distance/direction correlations. Travel distances were determined from a grid visible in the video frame. The grid-spacing distance was calibrated with a ruler placed in the focal plane, to account for perspective. Im-

probable trajectory segments were removed manually. For each no-flow replicate, we obtained between 100 and 300 larval trajectories. For each turbulence treatment replicate, we obtained several hundred to 2,000 trajectories. To use only independent velocity measurements, we took the velocity for a single frame-to-frame step from each trajectory, using the step beginning closest to the center of the video frame. A few outliers (<2% of the samples) were removed for the statistical analysis.

The software did introduce a potential bias by splitting crossed trajectories. Hovering and swimming larvae move more slowly than sinking larvae, and slow-moving larval tracks had more steps and a greater likelihood of being split. The result was an artificial increase in the number of measurements, particularly for hoverers and swimmers. Because this bias was unlikely to add support to our hypothesis, we considered it an acceptable observation error.

Analysis

Turbulence—To avoid disturbance of larvae during the experiments, we estimated turbulence characteristics from separate LDV measurements, from relationships of grid-tank dynamics, and from larval velocity measurements. LDV measurements were used to calculate the mean vertical flow velocity $\langle w \rangle$ and root-mean-square (rms) vertical velocity w', using unbiased approximations for a burst-sampled process (Buchave et al. 1979). The spectrum of the velocity time series was estimated with a block-averaged, discrete periodogram for randomly sampled data (Chan et al. 1998). We estimated the noise variance σ_n^2 and velocity variance $\hat{\sigma}_o^2$ contributions from the spectrum (Voulgaris and Trowbridge 1998). The spectral rms velocity $\hat{w}'$ is $\sim\hat{\sigma}_o^2$. Relationships of grid-tank dynamics were used to calculate the theoretical rms vertical velocity w'_{HT} using the formulation in Hopfinger and Toly (1976) with empirical constants given in McKenna (2000). This estimate of w'_{HT} is a function of grid geometry and forcing conditions and is linearly related to Re_{HT}. Larval velocity measurements were used to estimate statistically the fluid velocity variance (σ_o^2) during each replicate of the larval experiments. Maximum-likelihood estimates (MLEs) of rms velocity w'_{ML} ($=\sigma_o$) were obtained by fitting a normal mixture model to the larval velocities, as described in the following sections.

For each estimate of rms velocity, the turbulence dissipation rate ε was calculated as $\varepsilon = (w')^3\ell^{-1}$, where the eddy length scale ℓ was taken to be $\ell = 0.2z$, and z is the distance from the grid (Tennekes and Lumley 1972; McKenna 2000). The Kolmogorov length scale was estimated by $\eta = (\nu^3\varepsilon^{-1})^{0.25}$, where ν is the kinematic viscosity (Tennekes and Lumley 1972).

Larval behavior—Our goal was to determine how many larvae were sinking with retracted velums, because sinking was the only behavior that we expected to be associated with settlement. The proportion of sinkers could not be estimated simply by integrating over the proportion of observed negative (downward) velocities, however, because the observed larval velocities have both a behavioral component and a fluid transport component. A sinking larva can be carried upward by an eddy, resulting in an observed velocity in an upward (positive) direction. Even in still water, swimming and hovering larvae (swimmers that maintain a relatively constant position) move both upward and downward, making it impossible to classify larvae as sinkers on the basis of downward movement alone. Ideally, larvae with their velums retracted could be classified visually as sinkers, regardless of their velocities. At higher turbulence levels, though, motion blur in our video images prevented us from classifying larvae by visual inspection. Larvae could not be categorized individually into behavioral modes; instead, we analyzed larval behavior statistically, by fitting a normal mixture model to our larval velocity data to estimate the proportions of swimming, hovering, and sinking larvae.

In our analysis of larval behavior, several assumptions were made.

(1) Instantaneous flow velocities W_o are normal, with mean μ_o and variance σ_o^2.

$$W_o \sim N(\mu_o, \sigma_o^2)$$

(2) In still water, the vertical velocities W_i of larvae in a given behavioral mode are approximately normal, with means μ_i and variances σ_i^2.

$$W_i \sim N(\mu_i, \sigma_i^2),$$

$$i = \begin{cases} 1 \text{ swimmers} & (\mu_1 > 0,\ \sigma_1^2 \geq 1) \\ 2 \text{ hoverers} & (\mu_2 \leq 0,\ \sigma_2^2 \leq 1) \\ 3 \text{ sinkers} & (\mu_3 < 0,\ \sigma_3^2 \geq 1,\ |\mu_3| > \mu_1,\ |\mu_2|) \end{cases}$$

(3) Flow velocity and larval velocity are independent and additive—that is, relative larval velocity in flow W_{T^i} equals flow velocity W_o plus larval behavioral velocity W_i.

$$W_{T^i} = W_o + W_i \tag{1}$$

(4) Larval sinking and swimming abilities do not change significantly with flow conditions. Within a behavioral mode, W_i is not a function of W_o.

Assumption 1 has been validated in laboratory studies of grid-generated turbulence (Mouri et al. 2002), and our LDV velocity data were normally distributed. Assumption 2 was justified by analysis of larval velocities in still water (details follow). Assumption 3 is frequently used in studies of particle transport in turbulence (e.g., Reeks 1977), because inertial forces are negligible for particles with Reynolds number ≤1. Assumption 4 could not be directly verified but was considered to be reasonable given the experimental conditions. For ciliary swimmers, the speed of movement is directly proportional to the ciliary beat frequency, which is limited by viscosity and by salinity- and temperature-dependent biochemical rates (Chia et al. 1984; Podolsky and Emlet 1993; Young 1995). These seawater properties remained constant during our experiment, and there would have been no viscosity- or biochemical rate–related effects on larval swimming or hovering abilities. Larval swimming orientations can potentially be affected by velocity shear (Jonsson et al. 1991), but such an effect was not apparent in our experiments (see ''Discussion'' section).

Our assumptions place no constraints on behavioral changes from one mode to another. Within a given behavioral mode, the larval velocities are drawn from a fixed,

known distribution, but individual larvae can switch behavioral modes without restriction.

Mixture model for larval behavior in still water—We first estimated the velocity means μ_i, variances σ_i^2, and mixing proportions α_i of swimmers, hoverers, and sinkers in no-flow conditions by fitting a three-component normal mixture model to the still-water larval velocity distributions. The probability density of observed larval vertical velocity w_L was modeled as

$$P(w_L|\alpha_i, \mu_i, \sigma_i^2) = \sum_{i=1}^{3} \alpha_i p_i(w_L|\mu_i, \sigma_i^2) \quad (2)$$

where, for $i = (1, 2, 3)$,

$$p_i(w_L|\mu_i, \sigma_i^2) = \frac{1}{\sqrt{2\pi\sigma_i^2}} \exp\left[\frac{-(w_L - \mu_i)^2}{2\sigma_i^2}\right] \quad (3)$$

Maximum-likelihood parameter estimates of α_i, μ_i, and σ_i^2 were calculated using the expectation-maximization (EM) algorithm (McLachlan and Peel 2000).

In still water, the proportion of sinkers α_3 was too low (<0.03 in all replicates) to use MLEs of μ_3 and σ_3^2 to describe the sinking velocities. The fall velocities of dead larvae were approximately normal and were used as a proxy for the velocity distribution of live, actively sinking larvae with retracted velums. Although larvae can sink with extended velums by stopping ciliary motion, we observed that most larvae fully retracted their velums when sinking in turbulence. Given the predominance of velum retraction and the relatively small difference in velocities of the two types of sinkers (<10%; H. L. Fuchs unpubl. data), we included only sinkers with retracted velums in the model.

The variables μ_i and σ_i^2 characterize the behavioral velocities of swimming, hovering, and sinking larvae from each culture (Fig. 3a) and were used as known values (by assumption 4) in the analysis of larval behavior in turbulence. Normality of the modes was assessed using probability plots. We also estimated the behavioral velocity range as the difference between mean swimming and sinking velocities, calculated as $\Delta w_L = \mu_1 - \mu_3$ (Fig. 3a). Larger values of Δw_L indicate that larvae have more control over their vertical position in the water.

Mixture model for larval behavior in turbulence—We estimated the proportions α_{T^i} of swimmers, hoverers, and sinkers in each turbulence treatment by fitting a three-component, normal mixture model to the observed velocity distributions of larvae in turbulence. By assumption 3, the relative velocity of a larva in turbulence W_{T^i} is the sum of its behavioral velocity W_i and the fluid velocity W_o. The random variables W_{T^i} are distributed with normal probability densities p_{T^i}, with means and variances given by

$$\begin{aligned} \mu_{T^i} &= \mu_i + \mu_o \\ \sigma_{T^i}^2 &= \sigma_i^2 + \sigma_o^2 \end{aligned} \quad (4)$$

For each observed larval relative velocity w_L, the behavioral mode i of the observed larva was unknown, and the probability density of w_L in turbulence was modeled as

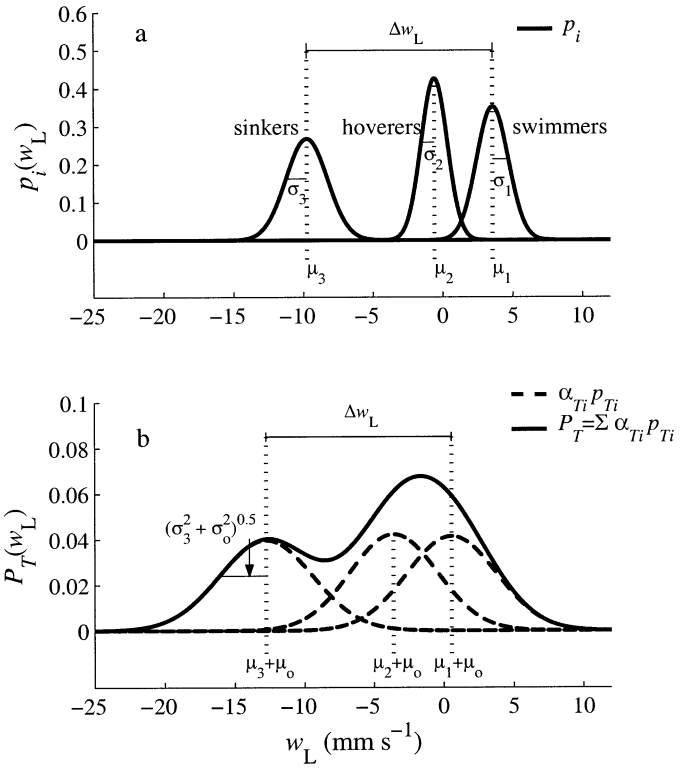

Fig. 3. Graphical representation of the three-component mixture model, showing the contribution of swimming, hovering, and sinking behaviors to the observed vertical velocity distribution of larvae in turbulence. (a) Behavioral velocity distributions of sinking, hovering, and swimming larvae were estimated for larvae in still water (dead larvae were used to determine sinking velocities) and were assumed to be independent of flow. Velocity means μ_i and SDs σ_i are indicated for each behavioral mode. (b) The three-component mixture model for observed larval velocity distributions in turbulence has contributions from each behavioral mode, where p_{T^i} are the probability densities of individual modes and α_{T^i} are the mixing proportions. Velocity means ($\mu_{T^i} = \mu_o + \mu_i$) are indicated for each behavioral component, the SD [$\sigma_{T^i} = \sqrt{(\sigma_o^2 + \sigma_i^2)}$] is indicated only for the sinking mode, and μ_o and σ_o^2 are the fluid velocity mean and variance. When the three-component mixture model was fitted to observed velocity data, α_{T^i} and σ_o were estimated by maximum likelihood. In this example, they were chosen arbitrarily for illustrative purposes ($\alpha_{T^i} = 0.\overline{33}$, $\mu_o = -3.0$ mm s^{-1}, $\sigma_o = 3.0$ mm s^{-1}, and $Re_{HT} = 100$). Note that because the mean flow velocity is negative, the model predicts that 77% of observed velocities would be <0 here, although the proportion of sinking larvae was only 33%.

$$P_T(w_L|\alpha_{T^i}, \mu_{T^i}, \sigma_{T^i}^2) = \sum_{i=1}^{3} \alpha_{T^i} p_{T^i}(w_L|\mu_{T^i}, \sigma_{T^i}^2) \quad (5)$$

(Fig. 3b). The mean flow velocity μ_o (=$\langle w \rangle$) from LDV measurements was used as a known value. By assumption 4, μ_i and σ_i^2 from still-water segments were also used as known values in eqs. 4 and 5. The unknown parameters (α_{T^i} and σ_o^2) were estimated for each treatment replicate using a modified EM algorithm (Web Appendix 1 at http://www.aslo.org/lo/toc/vol_49/issue_6/1937a1.pdf) to maximize the log-likelihood of eq. 5 over all observed velocities. Within the constraints of the model (eqs. 4, 5), σ_{T^i} has no statistical

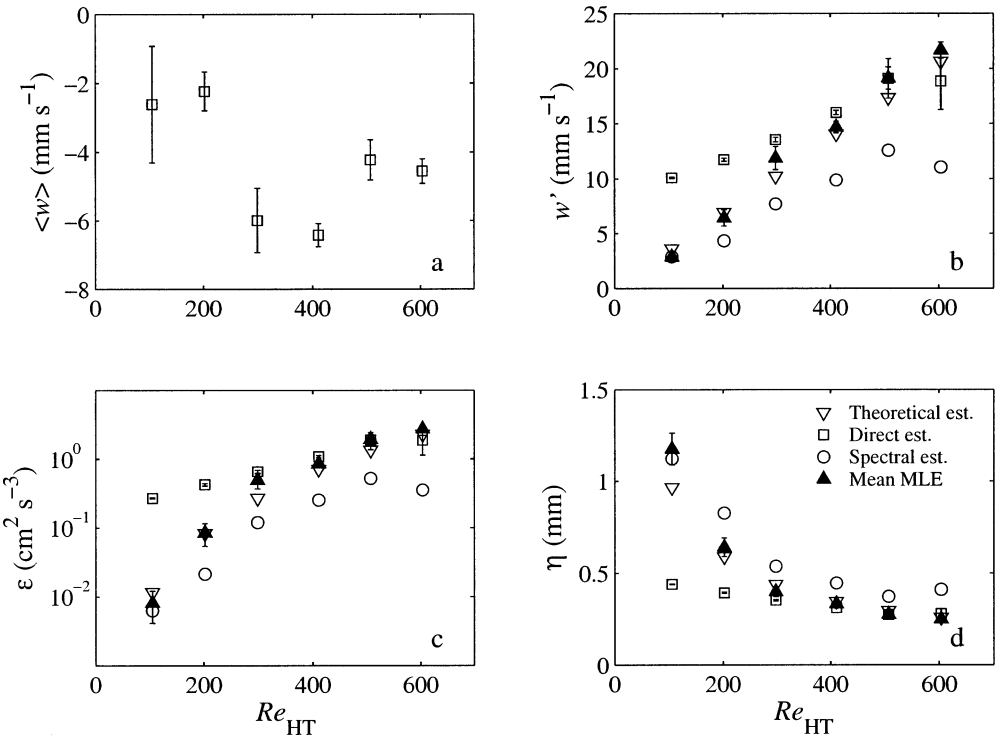

Fig. 4. Fluid velocity characteristics calculated from LDV measurements, from theory and from observed larval velocities. (a) Mean vertical velocity $\langle w \rangle$. (b) rms vertical velocity w'. (c) Turbulence dissipation rate ε. (d) Kolmogorov length scale η. Theoretical estimates were obtained using an empirical relationship between grid-forcing conditions and rms velocities (Hopfinger and Toly 1976). Direct, unbiased estimates were calculated from raw LDV data (Buchave et al. 1979). Spectral estimates were calculated by removing the estimated noise contribution from LDV velocity spectra (Voulgaris and Trowbridge 1998). MLEs were obtained by fitting a three-component mixture model to observed velocities of larvae in turbulence and averaging estimates from six replicates. Error bars are 1 SE. Mean flow velocity (a) cannot be estimated theoretically or by spectral methods.

dependence on σ_o^2, and these parameters can be estimated simultaneously from the observed larval velocities.

Relating behavior to turbulence—We wished to determine the general relationships between turbulence characteristics and the proportion of sinking larvae. Maximum-likelihood values of w'_{ML} ($=\sigma_o$ from the mixture model) were our best estimates of turbulence intensity in individual replicates (see ''Results'' section), and these were used to calculate the dissipation rate ε and the Kolmogorov length scale η for each turbulence treatment. The parameters were averaged by treatment level, and the relationships between ε or η and the proportion of sinkers σ_{T^3} were estimated by exponential regression.

Any group of larvae has a net mean behavioral velocity $\langle w_L \rangle$, and the relationship between $\langle w_L \rangle$ and ε is of interest for addressing population-level questions about larval fluxes. We calculated the net mean velocity of larvae in each treatment replicate as $\langle w_L \rangle = \sum \alpha_{T^i} \mu_i$. The relationship between $\langle w_L \rangle$ and $\log_{10}\varepsilon$,

$$\langle w_L \rangle = \mu_1 - a_0 e^{(a_1 \log_{10} \varepsilon)} \quad (6)$$

was estimated by exponential regression. The net velocity $\langle w_L \rangle$ is bounded above by the mean swimming velocity μ_1 and falls off exponentially with $\log_{10}\varepsilon$. Linear and logistic functions of ε were also fitted to $\langle w_L \rangle$ but had poorer fits and are omitted. Because larval swimming abilities varied among cultures, the model was fitted for individual replicates and for pooled data, excluding replicates with maximum and minimum values of Δw_L.

Results

Turbulence characteristics—A comparison of LDV measurements from five points in the video frame indicated that turbulence was generally homogeneous within our measurement area, although some inhomogeneities appeared at the highest turbulence level. At $Re_{HT} = 600$, w' values at the outer points differed from w' at the center point by 5–20%. In spite of this spatial inhomogeneity, we considered it worthwhile to present results from all turbulence treatment levels. All reported LDV results refer to the average of replicate measurements taken at the center point of the video frame.

The mean vertical flow velocity $\langle w \rangle$ was generally negative but always had a magnitude <7 mm s^{-1} (Fig. 4a). The relationship between Re_{HT} and mean flow velocity appeared to be nonlinear, presumably because the pattern of circulation in the tank has a nonlinear dependence on forcing conditions (McDougall 1979; McKenna 2000).

Table 3. Shell size and still-water velocities for competent larvae, given as mean ± 1 SD. Fall velocities were measured for a subsample of dead larvae ($n = 20$) from each replicate. Velocities were measured for live larvae ($100 < n < 300$) during each replicate, and the velocities of swimmers and hoverers and the mixing proportions were estimated by maximum likelihood. Also given is the mean difference between swimming velocity and fall velocity (Δw_L) for each culture.

Replicate	Age (days)	Shell length (μm)	Fall velocity (mm s^{-1})	Hovering velocity (mm s^{-1})	Swimming velocity (mm s^{-1})	Proportion of sinkers	Proportion of swimmers	Δw_L (mm s^{-1})
1	24	648±93	−9.2±1.1	−0.4±0.7	4.0±1.2	0.03	0.15	13.2
2	24	690±43	−9.2±1.0	−1.3±0.2	1.7±2.9	0.01	0.47	10.9
3	24	587±40	−6.4±1.2	−0.1±1.0	3.0±1.6	0.00	0.20	9.3
4	24	662±69	−8.8±1.5	−0.5±0.8	3.0±1.6	0.00	0.25	11.8
5	24	767±58	−9.8±1.5	−0.5±1.0	3.6±1.0	0.00	0.27	13.4
6	27	605±46	−7.0±1.2	−0.9±0.3	0.8±1.8	0.00	0.61	7.9

Direct estimates of w' increased linearly with Re_{HT} ($r^2 = 0.97$), from 10.1 mm s^{-1} at the lowest turbulence level to 18.9 mm s^{-1} at the highest level (Fig. 4b). Spectral estimates of $\hat{w}'$ were consistently ~7 mm s^{-1} less than direct estimates of w', indicating a substantial noise contribution in the measured velocity variance (Fig. 4b). The noise was assumed to have zero mean and no effect on $\langle w \rangle$. The spectral method sometimes overestimates the noise variance (Voulgaris and Trowbridge 1998), but LDV measurements are generally noisy because of Doppler noise and velocity shear in the measurement volume (Buchave et al. 1979; Voulgaris and Trowbridge 1998). Because of the high percentage of noise in the LDV measurements, the direct and spectral calculations were probably over- and underestimates of the rms velocity, but they are presented here as independent reference estimates.

When it was estimated from the three-component mixture model, the fluid velocity variance w'_{ML} was always close to the theoretical values w'_{HT} derived from empirical relationships of grid tank dynamics (Fig. 4b). This was also true for the turbulence dissipation rate ε (Fig. 4c) and Kolmogorov length scale η (Fig. 4d), which were calculated directly from rms velocity estimates. The close correspondence between our average estimates of w'_{ML} and w'_{HT} illustrates the validity of using a mixture model to estimate turbulence intensity by maximum likelihood from the measured larval velocities.

Because of uncertainty in w' and $\hat{w}'$ from the LDV measurements (due to the noise contribution) and because MLEs of w'_{ML} directly represent the turbulence intensity during each replicate of the larval experiments, we discuss our larval behavior results in terms of turbulence characteristics calculated from w'_{ML}. MLEs w'_{ML} closely resembled theoretical values w'_{HT}, and the relationships between larval behavior and w'_{ML} are qualitatively the same as those between behavior and w'_{HT}. As calculated from w'_{ML}, ε was 8.1×10^{-3}–2.7×10^{0} cm^2 s^{-3}, and η was 0.2–1.2 mm.

Larval velocities in still water—Although all larvae were raised under identical conditions, larval size and swimming abilities varied between cultures. Mean fall velocities were 6.4–9.8 mm s^{-1} (Table 3), and replicates 3 and 6 had significantly slower fall velocities than other replicates (one-way analysis of variance, $F_{5,114} = 24.268$, $p = 0.001$ with post-hoc Tukey's test). The slowest-sinking larvae were also the smallest, and larvae in replicate 6 had the slowest mean swimming velocity.

In no-flow conditions, hovering and swimming larvae formed two distinct groups in all replicates (Fig. 5a). Swimmers always had positive mean velocities and velocity variances >1 mm s^{-1}, whereas hoverers had negative mean velocities and velocity variances <1.1 mm s^{-1} (Table 3). The proportion of sinking larvae was always <0.03 and was $\ll$0.01 in four of six cultures. The proportions of swimming and hovering larvae varied between cultures. The behavioral velocity range Δw_L was 7.9–13.4 mm s^{-1}.

Larval behavior in turbulence—The distributions of observed larval velocities became wider at higher turbulence intensities (Fig. 5) because of the increased flow variance. The distributions also shifted toward more negative velocities at higher turbulence levels, in part because of the mean downward flow and in part because of the increasing proportion of sinking larvae. For larvae in still water, the velocity distributions were always positively skewed and bimodal, whereas in turbulence, the velocity distributions were negatively skewed.

We found a clear relationship between turbulence intensity and the proportion of larvae in each behavioral mode, as estimated from the three-component normal mixture model (Fig. 6). The proportion of sinking larvae was effectively zero at $Re_{HT} = 100$ and generally increased with turbulence intensity. The proportion of hovering larvae was lower in turbulence than in no-flow conditions. The proportion of swimming larvae was higher than other groups in turbulence up to $Re_{HT} = 400$ (e.g., Fig. 7) and then decreased at higher turbulence levels as the mean proportion of sinkers increased.

Relating behavior and turbulence—When data were averaged by turbulence treatment, the mean proportion of sinking larvae α_{T^3} increased approximately exponentially with the log of the dissipation rate [$\alpha_{T^3} = 0.26 \exp(1.1 \log_{10}\varepsilon)$, $r^2 = 0.89$; Fig. 8a] and decreased approximately exponentially with the Kolmogorov length scale [$\alpha_{T^3} = 0.71 \exp(-3.1\eta)$, $r^2 = 0.86$; Fig. 8b].

An exponential model provided a good fit ($r^2 = 0.73$ for pooled data) to the relationship between the net behavioral velocity $\langle w_L \rangle$ and the dissipation rate ε (Fig. 9). The net

behavioral velocity was negative at dissipation rates greater than $\varepsilon = 7.4 \times 10^{-2}$–$3.2 \times 10^{-1}$ cm^2 s^{-3}. When the data were pooled, this threshold was at 1.9×10^{-1} cm^2 s^{-3}.

Discussion

Mud snail veligers in our study altered their behavior in response to turbulent flow conditions and sank more frequently in more intense turbulence. Although we cannot show conclusively that veliger sinking behavior is a precursor to settlement, the response was demonstrated in late-stage, competent larvae. Moreover, the turbulence-induced response was most pronounced under turbulence conditions comparable to energetic nearshore areas where intertidal species must settle.

Our experimental turbulence treatments were specifically appropriate for questions about settlement in tidal flows at Barnstable Harbor, the natal habitat of our larvae. There are no published measurements of dissipation rates from the harbor, but Hunt and Mullineaux (2002) reported shear velocities of up to $u_* = 3.5$ cm s^{-1} over the inner-harbor tidal flats during flood tide. Using the relationship $\varepsilon = u_*^3/\kappa z$, where κ is von Karman's constant and z is height above bottom (Gross and Nowell 1985), the dissipation rate can be estimated as $\varepsilon \approx 10^0$ cm^2 s^{-3} over the flats. We measured turbulence in Barnstable Harbor during one complete tidal cycle in August 2002 and estimated dissipation rates to be $\varepsilon \approx 10^{-2}$–$10^1$ cm^2 s^{-3} (H. L. Fuchs unpubl. data). The lowest turbulence level used in our experiments ($\varepsilon = 8.1 \times 10^{-3}$ cm^2 s^{-3}) is probably representative of slack tide, whereas the higher turbulence levels (up to $\varepsilon = 2.7 \times 10^0$ cm^2 s^{-3}) would be found during flood or ebb tides. Although laboratory-generated turbulence is often more intense than that in relevant field conditions (Peters and Redondo 1997), our experimental turbulence levels were comparable to those in an adult mud snail habitat.

Our behavioral results (Fig. 8) suggest that veligers will exhibit sinking behavior in turbulent ($\varepsilon > 10^{-2}$ cm^2 s^{-3}), shallow areas but not in calmer ($\varepsilon < 10^{-2}$ cm^2 s^{-3}) offshore water. Our experiments were conducted at turbulence levels representative of tidal channels and partially mixed estuaries ($\varepsilon = 10^{-3}$–10^0 cm^2 s^{-3}; Table 1), where behavioral changes could potentially affect larval supply to intertidal habitats. Dissipation rates are generally lower in offshore areas and are unlikely to induce a larval sinking response, even during moderate storms. In winds ≈15 m s^{-1}, dissipation rates at the surface and thermocline reach $\varepsilon = 10^{-3}$–10^{-2} cm^2 s^{-3} (Dillon and Caldwell 1980), but our larvae rarely sank at $\varepsilon \leq 10^{-2}$ cm^2 s^{-3}. Although stormy conditions at sea could cause some veligers to sink (Barile et al. 1994), we expect that larvae will encounter and respond to strong turbulence primarily in nearshore areas.

Larval sinking in turbulent, coastal zones could potentially affect horizontal transport of larvae over spatial scales of tens of kilometers. Pringle and Franks (2001) described an asymmetric mixing mechanism that causes sinking particles to be transported shoreward in tidal currents. It is possible that physical mechanisms such as asymmetric mixing transport could enhance the retention of sinking larvae in coastal inlets, providing additional opportunities for settlement.

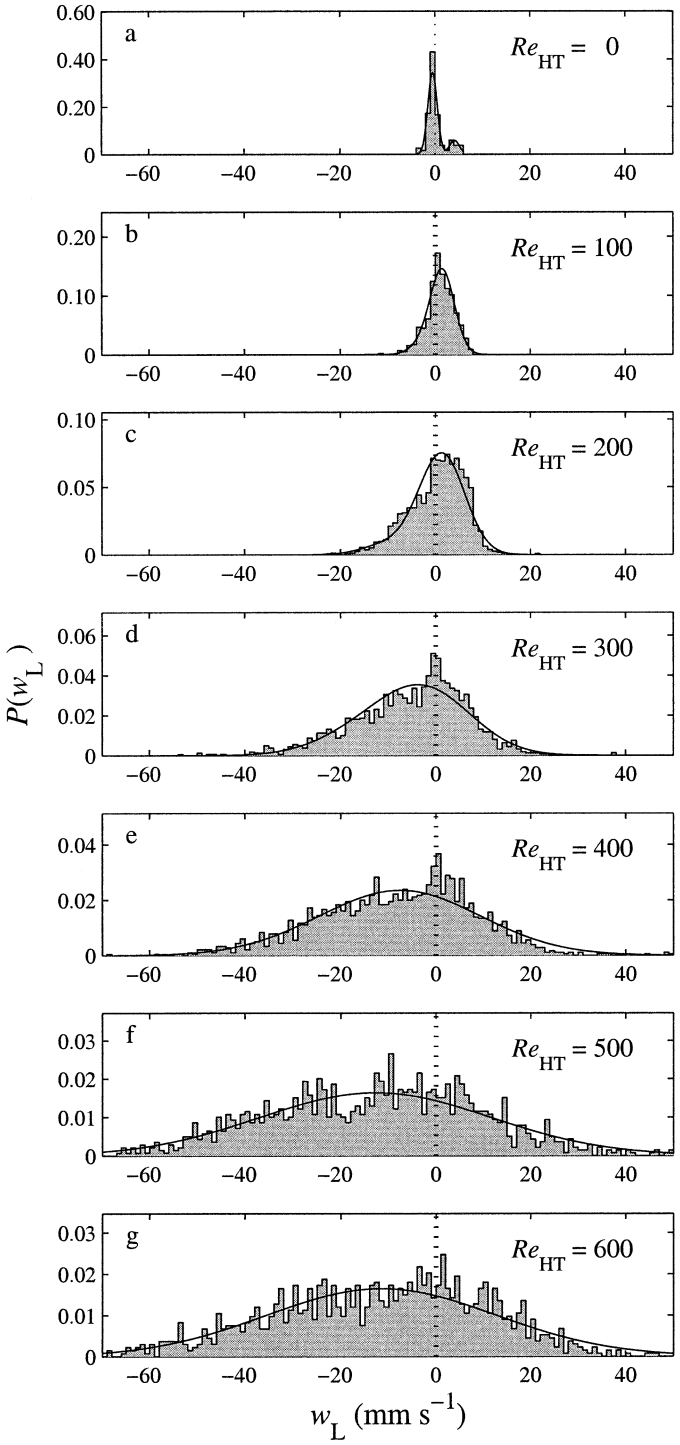

Fig. 5. Normalized histograms of observed larval vertical velocities for all turbulence levels, from replicate 1. Solid curves show the best fits from the three-component mixture model.

Larval behavior—We expected mud snail larvae to sink or swim, but we found that they also hover, especially in still water. Many species of mollusk larvae hover by producing mucous strings that act as natural tethers (Fenchel and Ockelmann 2002), but our larvae had no apparent mucous strings and were probably large and dense enough to

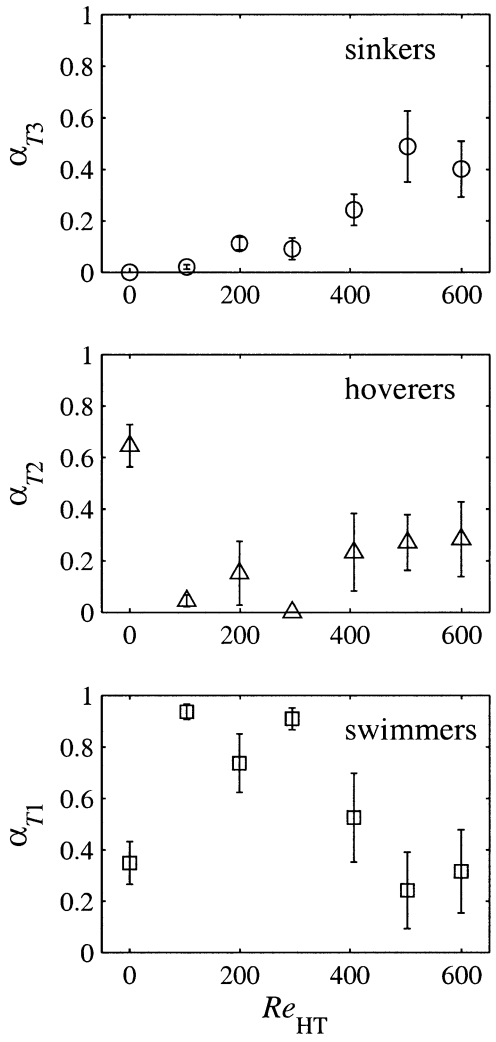

Fig. 6. Maximum-likelihood values of mean proportions α_{Ti} of sinking, hovering, and swimming larvae vs. Re_{HT}. Symbols show averaged estimates from all replicates for each turbulence treatment level. Error bars are 1 SE.

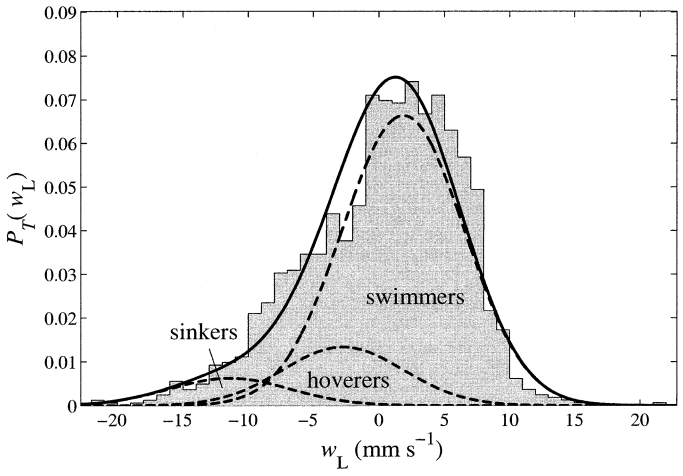

Fig. 7. Normalized histogram of observed larval velocities from replicate 1, Re_{HT} = 200, showing fitted velocity distribution for the three-component mixture model (solid curve) with contributions from each behavioral mode (dashed lines).

hover without added drag. Bivalve larvae create wider feeding currents and feed more efficiently by hovering than by swimming (Gallager 1993; Fenchel and Ockelmann 2002). In calm water, where contact rates between larvae and food particles are low, mud snail larvae also may hover more to increase feeding efficiency.

Larvae in our experiments sank more frequently at higher turbulence intensities, and this tendency could have important implications for settlement. Given constant turbulence conditions, sinking particles reach the bottom more quickly and accumulate to higher near-bottom concentrations than neutrally buoyant particles (e.g., McNair et al. 1997). Competent mud snail larvae would reach the benthos more quickly by sinking than by swimming, but there is no apparent benefit for larvae that sink in calm, deep water (e.g., offshore) over unsuitable habitats. The exponential relationship between the proportion of sinkers and $\log_{10}\varepsilon$ suggests that larvae should sink primarily in near-shore areas during en-

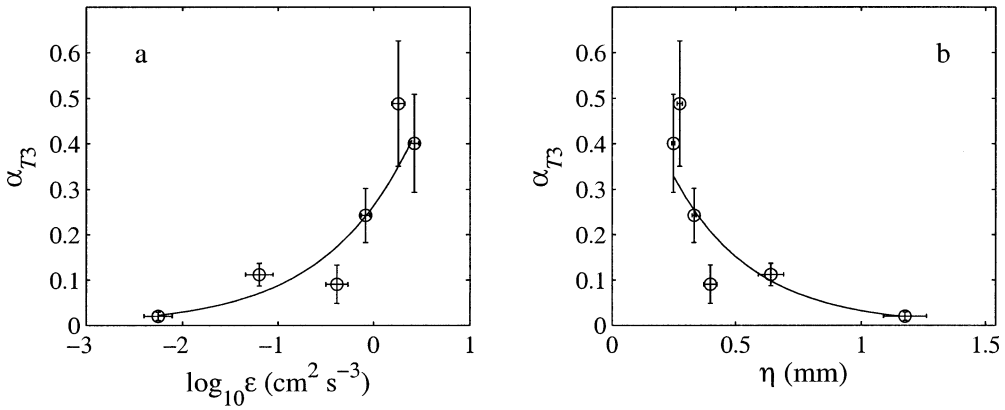

Fig. 8. Mean proportion of sinking larvae α_{T3} vs. (a) $\log_{10}$ of the dissipation rate ε and (b) Kolmogorov length scale η. All values are from MLEs. Symbols show average estimates from six replicates per treatment level (excluding Re_{HT} = 0), and error bars are 1 SE. Solid lines show exponential regressions.

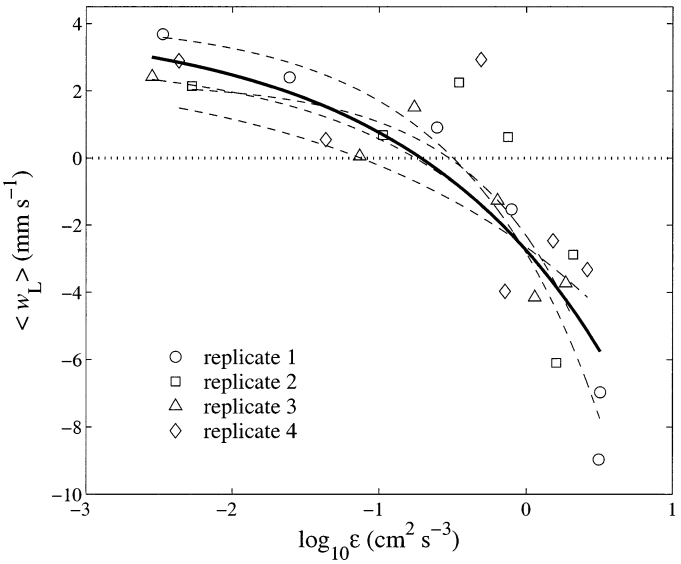

Fig. 9. Net mean behavioral velocity of larvae $\langle w_L \rangle$ vs. $\log_{10}$ of the dissipation rate ε. Symbols show velocity estimates for each treatment from replicates 1–4 (replicates with maximum and minimum values of Δw_L were excluded). Dashed lines show the exponential regressions for individual replicates, and the solid line shows the regression fit to pooled data, using $\mu_1 = 4.1$ mm s^{-1} and $\Delta w_L = 13.3$ mm s^{-1}.

ergetic tides, as might be expected if the response were related to settlement.

Veliger larvae clearly respond to turbulence, but the physiological mechanism of turbulence detection is unknown. Mud snail larvae retract their velums when the cilia are touched (Dickinson 2002), indicating the presence of mechanosensory cilia that could detect velocity shear. It has also been hypothesized that gastropod larvae sense acceleration with their statocysts (Chia et al. 1981; Crisp 1984; Young 1995). Chia et al. (1981) found a neural connection between the statocysts and cilia in nudibranch veligers (*Rostanga pulchra*), which suggests that these organs might have related functions. Both the velar cilia and the statocysts could potentially be used for detection of shear and acceleration in small eddies.

It is interesting to note that the sharpest increase in the proportion of sinking larvae occurred when the Kolmogorov length scale was less than the larval body length (Fig. 8b). Although Kolmogorov-scale eddies contain a very small percentage of the total turbulent kinetic energy, velocity gradients exist even at scales smaller than millimeters (Lazier and Mann 1989). Larvae may detect and respond to shear in the smallest-scale eddies, and sinking behavior could depend on interactions of larvae with eddies at the Kolmogorov scale. Alternatively, larvae may retract their velums in response to being accelerated or rotated by the flow vorticity, which increases with the dissipation rate. Regardless of the detection mechanism, descriptors of small-scale turbulence (η and ε) are probably the most relevant flow characteristics for understanding larval responses to turbulence.

Because vorticity increases with dissipation rate, velocity shear could potentially affect the orientation and directed-swimming abilities of larvae in strong turbulence. Larvae that normally swim in a velum-up orientation will begin to tumble if the viscous torque caused by velocity shear across the body greatly exceeds the gravitational torque, caused by an asymmetric density distribution. Tumbling is defined as rotation past 90° from the normal, velum-up orientation (Jonsson et al. 1991). We calculated the critical shear (as in Kessler 1986; Jonsson et al. 1991) required to tumble our larvae as $\text{shear}_{cr} \approx 10^2$ s^{-1}. This is about an order of magnitude greater than the highest shear rate in our experiments, which we estimated as shear $\approx \varepsilon^{0.5}\nu^{-0.5} = 1.6 \times 10^1$ s^{-1}. For shear $< 2 \times 10^1$ s^{-1}, the gravitational torque on the larvae will always compensate the viscous torque, allowing larvae to remain within about 10° of the normal upward orientation (Jonsson et al. 1991). Visual inspection of our video record confirmed that, even at the highest turbulence level, in-focus larvae were always oriented with the velums up. We conclude that velocity shear had little or no effect on larval swimming abilities in our experiment and that competent mud snail larvae probably tumble only in extremely turbulent conditions (e.g., the surf zone).

Implications of turbulence-induced sinking behavior—There are possible ecological and evolutionary benefits for veligers that sink in turbulence. Gastropod larvae may sink in turbulence as a way of avoiding predators (Young 1995). Mud snail veligers responded to turbulence even in the absence of predators, and we infer that larval fluxes are affected by turbulence-induced sinking behavior, regardless of whether turbulence is generated by predators or by physical sources. Abelson and Denny (1997) suggested that hydrodynamic forces might alter larval behavior and even provide a settlement cue. We hypothesize that a turbulence-induced sinking response enables larvae to move toward the bottom when they reach shallower coastal waters. Near-bottom larvae contact the bottom more frequently than those in the upper water column (McNair et al. 1997) and could have more opportunities to test substrates and settle in suitable areas.

To understand biophysical coupling between turbulence and settlement, it is necessary to determine the hydrodynamic conditions where larval behavior can affect sinking fluxes (Crimaldi et al. 2002). The net behavioral velocity of our larvae shifted from positive (upward) to negative (downward) when the dissipation rate reached $\sim\varepsilon = 10^{-1}$ cm^2 s^{-3}. This shift could result in significant changes in the advective component of larval vertical fluxes. On the other hand, the observed velocity distributions of our larvae grew wider as w' increased, indicating that larval movement is dominated more by flow as turbulence intensifies. Larvae probably detect eddies at or near the Kolmogorov scale, which is a function of ε, and we expect the proportion of sinking larvae α_{T^3} to increase exponentially with $\log_{10}\varepsilon$ in the field as in the lab. Behavioral changes may affect sinking fluxes less, however, when the vertical turbulence intensity w' greatly exceeds the behavioral velocity range Δw_L.

Although we focused on water-column processes, it is worth noting that settlement fluxes depend on both the probability of reaching the bottom and the probability of attachment to substrates (Gross et al. 1992; Crimaldi et al. 2002).

Like the dissipation rate, Reynolds stress increases with shear velocity, and those flow conditions that induce larval sinking are also more likely to cause bed-load transport or saltation of sediments and to prevent larvae from attaching to the bottom. In energetic flows such as the strong tides at Barnstable Harbor, a large proportion of competent larvae could be sinking at a given time (Fig. 8), concentrating nearer to the bottom than nonsinking larvae do. Although the probability of larval attachment to substrates is lower in the higher shear stresses of turbulent flows (Gross et al. 1992; Pawlik and Butman 1993), near-bottom larvae could have more opportunities to test substrates and burrow into sediments during slack tides (tens of minutes) or brief lulls in turbulence (seconds to minutes; Crimaldi et al. 2002).

Turbulence varies spatially and temporally in coastal areas, and large-scale settlement patterns could be influenced by flow-mediated, active settlement processes rather than by passive deposition alone. Our motivation is to understand how biophysical coupling between turbulence and settlement behavior affects the supply of gastropod larvae to coastal populations. We have shown that turbulence alters the behavior of competent mud snail larvae in the laboratory. Field and modeling studies are in progress to determine how this biophysical coupling affects larval supply and settlement fluxes of intertidal gastropods.

References

ABELSON, A., AND M. DENNY. 1997. Settlement of marine organisms in flow. Annu. Rev. Ecol. Syst. **28:** 317–339.

BARILE, P. J., A. W. STONER, AND C. M. YOUNG. 1994. Phototaxis and vertical migration of the queen conch (*Strombus gigas* linne) veliger larvae. J. Exp. Mar. Biol. Ecol. **183:** 147–162.

BUCHAVE, P., W. K. GEORGE, JR., AND J. L. LUMLEY. 1979. The measurement of turbulence with the laser-Doppler anemometer. Annu. Rev. Fluid Mech. **11:** 443–503.

BUTMAN, C. A. 1987. Larval settlement of soft-sediment invertebrates: The spatial scales of pattern explained by active habitat selection and the emerging role of hydrodynamical processes. Oceanogr. Mar. Biol. Annu. Rev. **25:** 113–165.

CHAN, N. H., J. B. KADANE, AND T. JIANG. 1998. Time series analysis of diurnal cycles in small-scale turbulence. Environmetrics **9:** 235–244.

CHIA, F.-S., J. BUCKLAND-NICKS, AND C. M. YOUNG. 1984. Locomotion of marine invertebrate larvae: A review. Can. J. Zool. **62:** 1205–1222.

———, R. KOSS, AND L. R. BICKELL. 1981. Fine structural study of the statocysts in the veliger larva of the nudibranch, *Rostanga pulchra*. Cell Tissue Res. **214:** 67–80.

CRIMALDI, J. P., J. K. THOMPSON, J. H. ROSMAN, R. J. LOWE, AND J. R. KOSEFF. 2002. Hydrodynamics of larval settlement: The influence of turbulent stress events at potential recruitment sites. Limnol. Oceanogr. **47:** 1137–1151.

CRISP, D. J. 1984. Overview of research on marine invertebrate larvae, 1940–1980, p. 103–127. *In* J. D. Costlow, and R. C. Tipper [eds.], Marine biodeterioration: An interdisciplinary study. Naval Institute Press.

DE SILVA, I. P. D., AND H. J. S. FERNANDO. 1994. Oscillating grids as a source of nearly isotropic turbulence. Phys. Fluids **6:** 2455–2464.

DICKINSON, A. J. G. 2002. Neural and muscular development in a gastropod larva. Ph.D. thesis, Dalhousie Univ.

DILLON, T. M., AND D. R. CALDWELL. 1980. The Batchelor spectrum and dissipation in the upper ocean. J. Geophys. Res. **85:** 1910–1916.

ECKMAN, J. E., F. E. WERNER, AND T. F. GROSS. 1994. Modelling some effects of behavior on larval settlement in a turbulent boundary layer. Deep-Sea Res. II **41:** 185–208.

FENCHEL, T., AND K. W. OCKELMANN. 2002. Larva on a string. Ophelia **56:** 171–178.

GALLAGER, S. M. 1993. Hydrodynamic disturbances produced by small zooplankton: Case study for the veliger larva of a bivalve mollusc. J. Plankton Res. **15:** 1277–1296.

GEORGE, R., R. E. FLICK, AND R. T. GUZA. 1994. Observations of turbulence in the surf zone. J. Geophys. Res. **99:** 801–810.

GROSS, T. F., AND A. R. M. NOWELL. 1985. Spectral scaling in a tidal boundary layer. J. Phys. Oceanogr. **15:** 496–508.

———, F. E. WERNER, AND J. E. ECKMAN. 1992. Numerical modeling of larval settlement in turbulent bottom boundary layers. J. Mar. Res. **50:** 611–642.

HIDU, H., AND H. H. HASKIN. 1978. Swimming speeds of oyster larvae *Crassostrea virginica* in different salinities and temperatures. Estuaries **1:** 252–255.

HOPFINGER, E. J., AND J.-A. TOLY. 1976. Spatially decaying turbulence and its relation to mixing across density interfaces. J. Fluid Mech. **78:** 155–175.

HUNT, H. L., AND L. S. MULLINEAUX. 2002. The roles of predation and postlarval transport in recruitment of the soft shell clam (*Mya arenaria*). Limnol. Oceanogr. **47:** 151–164.

JONSSON, P. R., C. ANDRÉ, AND M. LINDEGARTH. 1991. Swimming behaviour of marine bivalve larvae in a flume boundary-layer flow: Evidence for near-bottom confinement. Mar. Ecol. Progr. Ser. **79:** 67–76.

KESSLER, J. O. 1986. The external dynamics of swimming microorganisms. Prog. Phycol. Res. **4:** 257–291.

LAZIER, J. R. N., AND K. H. MANN. 1989. Turbulence and the diffusive layers around small organisms. Deep-Sea Res. Part A **36:** 1721–1733.

MACKENZIE, B. R., AND T. KIØRBOE. 1995. Encounter rates and swimming behavior of pause-travel and cruise larval fish predators in calm and turbulent laboratory environments. Limnol. Oceanogr. **40:** 1278–1289.

MCDOUGALL, T. J. 1979. Measurements of turbulence in a zero-mean-shear mixed layer. J. Fluid Mech. **94:** 409–431.

MCKENNA, S. P. 2000. Free-surface turbulence and air-water gas exchange. Ph.D. thesis, MIT/WHOI Joint Program.

MCLACHLAN, G., AND D. PEEL. 2000. Finite mixture models. Wiley.

MCNAIR, J. N., J. D. NEWBOLD, AND D. D. HART. 1997. Turbulent transport of suspended particles and dispersing benthic organisms: How long to hit bottom? J. Theor. Biol. **188:** 29–52.

MOURI, H., M. TAKAOKA, A. HORI, AND Y. KAWASHIMA. 2002. Probability density function of turbulent velocity fluctuations. Phys. Rev. E **65.** [doi: 10.1103/PhysRevE.65.056304].

OAKEY, N. S., AND J. A. ELLIOTT. 1982. Dissipation within the surface mixed layer. J. Phys. Oceanogr. **12:** 171–185.

PAWLIK, J. P. 1992. Chemical ecology of the settlement of benthic marine invertebrates. Oceanogr. Mar. Biol. Annu. Rev. **30:** 273–335.

———, AND C. A. BUTMAN. 1993. Settlement of a marine tube worm as a function of current velocity: Interacting effects of hydrodynamics and behavior. Limnol. Oceanogr. **38:** 1730–1740.

PETERS, F., AND J. M. REDONDO. 1997. Turbulence generation and measurement: Application to studies on plankton. Sci. Mar. **61(Suppl. 1)**: 205–228.

PODOLSKY, R. D., AND R. B. EMLET. 1993. Separating the effects of temperature and viscosity on swimming and water movement by sand dollar larvae (*Dendraster excentricus*). J. Exp. Biol. **176:** 207–221.

PRINGLE, J. M., AND P. J. S. FRANKS. 2001. Asymmetric mixing transport: A horizontal transport mechanism for sinking plankton. Limnol. Oceanogr. **46:** 381–391.

REEKS, M. W. 1977. On the dispersion of small particles suspended in an isotropic turbulent fluid. J. Fluid Mech. **83:** 529–546.

SAIZ, E. 1994. Observations of the free-swimming behavior of *Acartia tonsa:* Effects of food concentration and turbulent water motion. Limnol. Oceanogr. **39:** 1566–1578.

SCHELTEMA, R. S. 1961. Metamorphosis of the veliger larvae of *Nassarius obsoletus* (Gastropoda) in response to bottom sediment. Biol. Bull. **120:** 92–109.

———, I. P. WILLIAMS, M. A. SHAW, AND C. LOUDON. 1981. Gregarious settlement by the larvae of *Hydroides dianthus* (Polychaeta: Serpulidae). Mar. Ecol. Prog. Ser. **5:** 69–74.

SNELGROVE, P. V. R., J. P. GRASSLE, AND C. A. BUTMAN. 1998. Sediment choice by settling larvae of the bivalve, *Spisula solidissima* (Dillwyn), in flow and still water. J. Exp. Mar. Biol. Ecol. **231:** 171–190.

TAMBURRI, M. N., C. M. FINELLI, D. S. WETHEY, AND R. K. ZIMMER-FAUST. 1996. Chemical induction of larval settlement behavior in flow. Biol. Bull. **191:** 367–373.

TENNEKES, H., AND J. L. LUMLEY. 1972. A first course in turbulence. MIT Press.

VOULGARIS, G., AND J. H. TROWBRIDGE. 1998. Evaluation of the acoustic Doppler velocimeter (ADV) for turbulence measurements. J. Atmos. Ocean. Technol. **15:** 272–289.

WELCH, J. M., AND R. B. FORWARD, JR. 2001. Flood tide transport of blue crab, *Callinectes sapidus,* postlarvae: Behavioral responses to salinity and turbulence. Mar. Biol. **139:** 911–918.

YOUNG, C. M. 1995. Behavior and locomotion during the dispersal phase of larval life, p. 249–278. *In* L. McEdward [ed.], Ecology of marine invertebrate larvae. CRC Press.

Received: 30 January 2004
Accepted: 6 July 2004
Amended: 19 July 2004